Precision determination of the small-x gluon from charm production at LHCb

Rhorry Gauld[1, 2, *] and Juan Rojo[3, 4, †]

[1] Institute for Theoretical Physics, ETH, CH-8093 Zurich, Switzerland
[2] Institute for Particle Physics Phenomenology, University of Durham, DH1 3LE Durham, United Kingdom
[3] Department of Physics and Astronomy, VU University Amsterdam,
De Boelelaan 1081, NL-1081, HV Amsterdam, The Netherlands
[4] Nikhef, Science Park 105, NL-1098 XG Amsterdam, The Netherlands
(Dated: June 26, 2017)

The small-x gluon in global fits of parton distributions is affected by large uncertainties from the lack of direct experimental constraints. In this work we provide a precision determination of the small-x gluon from the exploitation of forward charm production data provided by LHCb for three different centre-of-mass (CoM) energies: 5 TeV, 7 TeV and 13 TeV. The LHCb measurements are included in the PDF fit by means of normalized distributions and cross-section ratios between data taken at different CoM values, $R_{13/7}$ and $R_{13/5}$. We demonstrate that forward charm production leads to a reduction of the PDF uncertainties of the gluon down to $x \simeq 10^{-6}$ by up to an order of magnitude, with implications for high-energy colliders, cosmic ray physics and neutrino astronomy.

The determination of the internal structure of the proton, as encoded by the non-perturbative parton distribution functions (PDFs) [1–3], has far-reaching implications for many areas in nuclear, particle and astroparticle physics. A topic that has recently attracted substantial interest is the determination of the gluon PDF at small-x, which is of direct relevance for the modelling of soft QCD at the LHC [4], neutrino astronomy [5–8] and cosmic ray physics [9], as well as for future lepton-proton [10] and proton-proton higher-energy colliders [11]. Constraints on the gluon PDF from deep-inelastic scattering (DIS) inclusive and charm structure functions at HERA [12, 13] are limited to $x \gtrsim 3 \cdot 10^{-5}$ in the perturbative region, and consequently for smaller values of x there are large uncertainties from the lack of direct experimental information.

Last year, it was realized [14–16] that a way forward was provided by considering inclusive D meson production in pp collisions at the LHC, for which the LHCb experiment had already provided data at 7 TeV [17]. The inclusive charm cross-section at the LHC is dominated by heavy quark pair production, in turn driven by the gluon-gluon luminosity, and the forward LHCb kinematics allow a coverage of the small-x region that can reach as low as $x \simeq 10^{-6}$. While the direct inclusion of absolute D meson cross-sections into a PDF fit is unfeasible due to the large theory uncertainties that affect the NLO calculation, it has been demonstrated [14, 15] that by using tailored normalized distributions it is possible to exploit the LHCb measurements to achieve a significantly improved description of the small-x gluon. A complementary approach, suggested in [16], would be to include D meson data into PDF fits with the use of ratios of cross-sections between different center-of-mass (CoM) energies,

which benefit from various uncertainty cancellations [18].

More recently, the LHCb collaboration has presented the analogous D meson cross-section measurements at $\sqrt{s} = 5$ and 13 TeV [19, 20], together with the corresponding ratios $R_{13/7}$ and $R_{13/5}$.[1] In this letter, we quantify the impact of the LHCb D meson data at different CoM energies on the small-x gluon from the NNPDF3.0 global analysis [21]. These data are included both in terms of normalized cross-sections as well as by means of the cross-section ratio measurements. Our strategy leads to a precision determination of the small-x gluon, substantially improving previous results, and highlighting the consistency of the LHCb measurements at the three CoM energies. We illustrate the implications of our results for ultra high-energy (UHE) neutrino-nucleus cross-sections $\sigma_{\nu N}(E_\nu)$, and the longitudinal structure function $F_L(x, Q^2)$ at future lepton-proton colliders.

The LHCb D meson production data is presented double differentially in transverse momentum (p_T^D) and rapidity (y^D) for a number of final states, D^0, D^+, D_s^+ and D^{*+}, which also contain the contribution from charge-conjugate states. To include these measurements into the global PDF fit, we define two observables:

$$N_X^{ij} = \frac{d^2\sigma(\text{X TeV})}{dy_i^D d(p_T^D)_j} \bigg/ \frac{d^2\sigma(\text{X TeV})}{dy_{\text{ref}}^D d(p_T^D)_j}, \qquad (1)$$

$$R_{13/X}^{ij} = \frac{d^2\sigma(13 \text{ TeV})}{dy_i^D d(p_T^D)_j} \bigg/ \frac{d^2\sigma(\text{X TeV})}{dy_i^D d(p_T^D)_j}, \qquad (2)$$

which benefit from the partial cancellation of the residual scale dependence from missing higher-orders, while retaining sensitivity to the gluon since different regions of x are probed in the numerator and denominator of

*Electronic address: rgauld@phys.ethz.ch
†Electronic address: j.rojo@vu.nl

[1] The LHCb 5 and 13 TeV data considered here corresponds to the update provided in May 2017.

these observables. The ratio measurements, $R_{13/7}$ and $R_{13/5}$, are available for $y^D \in [2.0, 4.5]$ in five bins and for $p_T^D \in [0, 8]$ GeV in eight bins. The 5 TeV and 13 TeV absolute cross section measurements extend to higher p_T^D values, however these additional points are excluded from the fit since they might be affected by large logarithmic contributions [22]. In this way, data in a fixed kinematic region is included either through cross-section ratios or normalized cross-sections. The reference rapidity bin in the normalized distributions N_X^{ij} in Eq. (1) is chosen to be $y_{\text{ref}}^D \in [3.0, 3.5]$, as in [15], since we have verified that this choice maximizes the cancellation of scale uncertainties for the considered data. We restrict our analysis to the $\{D^0, D^+, D_s^+\}$ final states, ignoring that of D^{+*} which has an overlapping contribution with that of D^0 and D^+.

The theoretical predictions for D meson production are computed at NLO+PS accuracy using POWHEG [23–25] to match the fixed-order calculation [26] to the PYTHIA8 shower [27, 28] with the MONASH 2013 tune [4]. The POWHEG results have previously been shown to be consistent [14, 29] with both the NLO+PS (a)MC@NLO [30, 31] method and the semi-analytic FONLL calculation [32, 33]. The NNPDF3.0 NLO set of parton distributions with $\alpha_s(m_Z) = 0.118$, $N_f = 5$ and $N_{\text{rep}} = 1000$ replicas has been used, interfaced with LHAPDF6 [34]. The internal POWHEG routines have been modified to extract α_s from LHAPDF6, and the compensation terms [32] to consistently match the $N_f = 5$ PDFs with the fixed-order $N_f = 3$ calculation [26] are included. The central value for the charm quark pole mass is taken to be $m_c = 1.5$ GeV, following the HXSWG recommendation [35], and the renormalization and factorization scales are set equal to the heavy quark transverse mass in the Born configuration, $\mu = \mu_R = \mu_F = \sqrt{m_c^2 + p_T^2}$.

Other settings of the theory calculation, such as the values for fragmentation fractions, are the same as those in [14]. We have verified that the choice of PYTHIA8 tune (comparing MONASH 2013 with 4C or A14) as well as the modelling of charm fragmentation (using for $e.g.$ a Peterson function with $\epsilon_D = 0.05$ and varying ϵ_D by a factor 2) on the observables of Eq. (1) leads in all cases to variations that are negligible as compared to PDF uncertainties.

The impact of the LHCb D meson data on the NNPDF3.0 small-x gluon can be quantified using the Bayesian reweighting technique [36, 37]. We have studied separately the impact of the three data sets of normalized distributions, N_5, N_7 and N_{13} and the two cross-section ratios, $R_{13/5}$ and $R_{13/7}$, as well specific combinations of these, always avoiding double counting. The experimental bin-by-bin correlation matrices are included for the cross-section ratios $R_{13/X}$, while for the normalized cross-section data the (cross-section level) bin-by-bin correlations, which are only available for N_5 and N_{13}, are not included.

We find that NLO theory describes successfully both the cross-section ratios $R_{13/7}$ and $R_{13/5}$ as well as the normalized cross section data at all three CoM energies. To illustrate this agreement, we compute the χ^2/N_{dat} for each of the five datasets, for different combinations of data used as input in the PDF fit. These results are summarized in Table I, where the data that has been included in each case are highlighted in boldface, and the number in brackets indicates N_{dat} for each data set. For example, the first row corresponds to the baseline PDF set, the second row indicates the resultant χ^2/N_{dat} for each data set after the N_5 data has been added to NNPDF3.0, and so on.

$N_5(84)$	$N_7(79)$	$N_{13}(126)$	$R_{13/5}(107)$	$R_{13/7}(102)$
1.97	1.21	2.36	1.36	0.80
0.86	0.72	1.14	1.35	0.81
1.31	**0.91**	1.58	1.36	0.82
0.74	0.66	**1.01**	1.38	0.80
1.08	0.81	1.27	**1.29**	0.80
1.53	0.99	1.73	1.30	**0.81**
1.07	0.81	1.34	1.35	**0.81**
0.82	**0.70**	1.07	**1.35**	0.81
0.84	**0.71**	**1.10**	1.36	0.81

TABLE I: The χ^2/N_{dat} for the LHCb D meson measurements considered, N_5, N_7, N_{13}, $R_{13/7}$ and $R_{13/5}$, for various combinations of input to the PDF fit (highlighted in boldface).

We find that the normalized distributions, N_5, N_7 and N_{13}, as well as the ratio $R_{13/5}$, have a similar substantial pull on the gluon, both for central values and for the reduction of the PDF uncertainty. It is found that the $R_{13/7}$ ratio data has only a minor impact on the central value and resultant uncertainty of the small-x gluon. This can in part be understood due to the fact that this data is less precise in comparison to the $R_{13/5}$ data, and additionally less sensitive to the rate of change of the gluon PDF at low-x. We find it reassuring that including each of the available LHCb data sets to NNPDF3.0, one at a time, improves the description of all other data sets. In Fig. 1 we show the 1-σ relative PDF uncertainties for the gluon at $Q^2 = 4$ GeV^2 in NNPDF3.0 and in the subsequent fits when the various LHCb D meson data sets are included.

In the following we show results for two representative combinations of the LHCb measurements, namely $N_7 + R_{13/5}$ and $N_5 + N_7 + N_{13}$. In Fig. 2 we compare the small-x gluon in NNPDF3.0 with the resultant gluon in these two cases, as well as the central value from the $N^5 + R^{13/7}$ fit. The central value of the small-x gluon is consistent for all three combinations, down to $x \simeq 10^{-6}$, and, as expected from Fig. 1, we observe a dramatic reduction of the 1-σ PDF uncertainties. We have verified that these updated results are consistent with our original study [14]
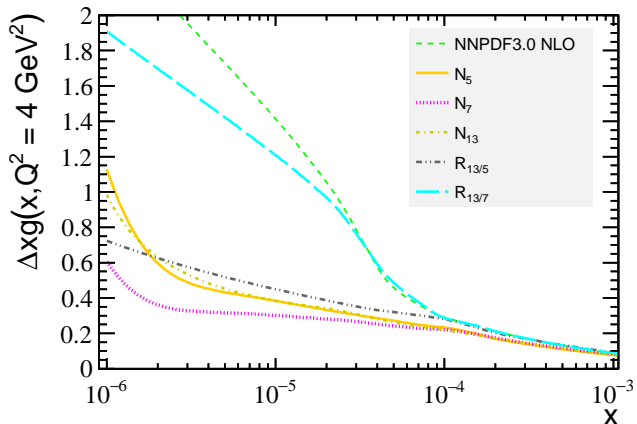
FIG. 1: The 1-σ relative PDF uncertainties for the small-x gluon at $Q^2 = 4$ GeV^2 in NNPDF3.0 and in the subsequent fits when the LHCb charm data are included one at a time.

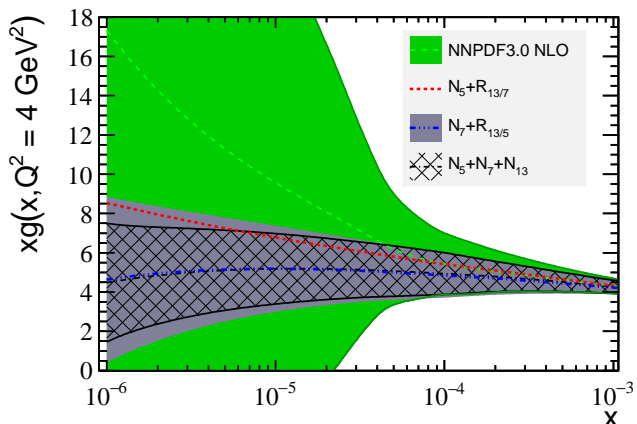(GRRT), yet significantly more precise, as demonstrated in Fig. 5.

FIG. 2: The NLO gluon in NNPDF3.0 and for various combinations of LHCb data included, at $Q^2 = 4$ GeV^2.

Given the sizeable theory errors that affect charm production, it is important to assess the robustness of our results with respect to the scale variations of the NLO calculation as well as with the value of m_c. We thus have quantified how the resultant gluon are affected by theory variations, including: $\mu = \sqrt{4m_c^2 + p_T^2}$, as well as charm mass variations of $\Delta m_c = 0.2$ GeV. An additional check of applying a minimum p_T requirement of 2 GeV to the cross section data was also performed, which had little impact and is not shown. The resultant central values of the gluon are shown in Figs. 3 and 4, compared with NNPDF3.0 and with the 1-σ PDF uncertainty band from the $N_5 + N_7 + N_{13}$ and $N_7 + R_{13/5}$ fits, respectively.

We find that our results are reasonably stable upon these variations of the input theory settings, in particular for the $N^7 + R^{13/5}$ fits, highlighting that the cancellation of theory errors is more effective for the cross-section ratios than for the normalized distributions. Even
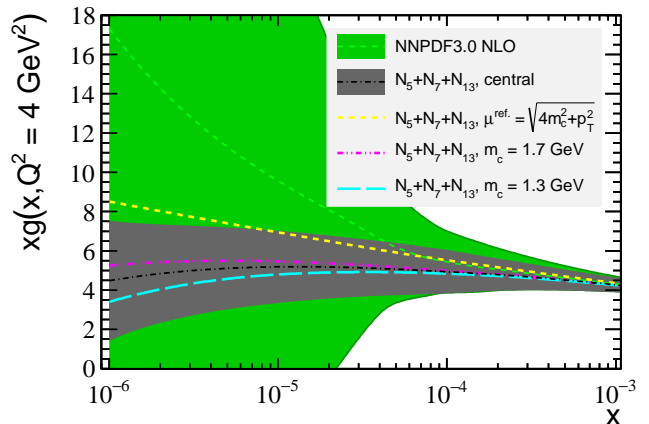

FIG. 3: Dependence of the small-x gluon from the $N_5 + N_7 + N_{13}$ fits for variations in the input theory settings.

for the most constraining combination, corresponding to $N_5 + N_7 + N_{13}$, all theory variations are contained within the 95% confidence level interval of the PDF uncertainty. This study demonstrates that the sizeable reduction of the small-x gluon PDF errors is robust with respect to theoretical uncertainties. A further reduction of the scale dependence could only be achieved by the full NNLO calculation, so far available only for $t\bar{t}$ production [38].
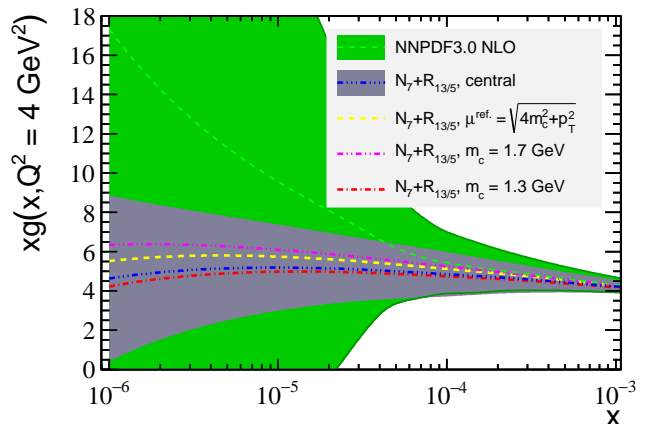

FIG. 4: Same as Fig. 3 for the $N^7 + R^{13/5}$ fits.

Our precision determination of the small-x gluon has important phenomenological implications, which we choose to illustrate with two representative examples: the longitudinal structure function F_L at a future high-energy lepton-proton collider, and the UHE neutrino-nucleus cross-section. First of all, we have computed $F_L(x, Q^2)$ for $Q^2 = 3.5$ GeV^2 using APFEL [39] in the FONLL-B general mass scheme [40]. The proposed Large Hadron electron Collider (LHeC) would be able to measure to measure F_L down to $x \gtrsim 10^{-6}$ with few percent precision for $Q^2 \gtrsim 2$ GeV^2 [10], hence providing a unique probe of BFKL resummations and non-linear QCD dynamics [41]. In Fig. 5 we compare F_L computed with NNPDF3.0 and with the results of this work, as well as

with the original GRRT calculation. We observe that the PDF uncertainties on F_L at $x \simeq 10^{-6}$ are now reduced by around a factor of 5 with respect to the baseline, and that F_L itself is always positive for the x range accessible at the LHeC.
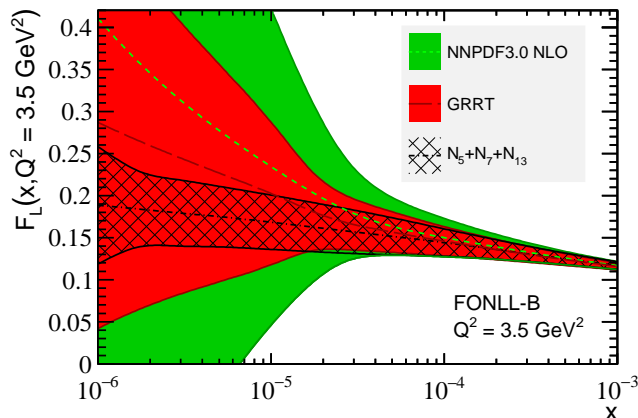

FIG. 5: The structure function $F_L(x, Q^2)$ at $Q^2 = 3.5$ GeV^2, comparing the NNPDF3.0 predictions both with the results of this work and with the GRRT calculation.

Next, we have computed the UHE charged-current (CC) neutrino-nucleus cross-section as a function of the incoming neutrino energy E_ν, using a stand-alone code based on APFEL for the calculation of the NLO structure functions. At the highest values of E_ν that might be accessible at neutrino telescopes such as IceCube [42] and KM3NET [43], the neutrino-nucleus interactions probes the quark sea PDFs at $Q^2 \simeq M_W^2$ and down to $x \simeq 10^{-8}$, a region where the quark distributions are driven by the small-x gluon by means of DGLAP evolution effects [44].

In Fig. 6 we compare the CC UHE neutrino-nucleus cross-section from NNPDF3.0 with the results of this work. As in the case of F_L, we find a sizeable reduction of the PDF uncertainties, which are by far the dominant theory uncertainty for this process at high E_ν. This way, NLO QCD provides a prediction accurate to $\lesssim 10\%$ up to $E_\nu \simeq 10^{12}$ GeV, a region where a rather different behaviour are found in scenarios with non-linear QCD evolution effects [45]. Our results for the UHE cross-section are more precise than existing calculations [46], based on PDF fits where the only constraints on the small-x gluon come from the inclusive and charm HERA data, and therefore provide a clean handle to disentangle possible beyond the Standard Model effects in this process [47].

To summarize, in this work we have presented a precision determination of the small-x gluon down to $x \simeq 10^{-6}$ from LHCb charm production in the forward region at $\sqrt{s} =$ 5, 7 and 13 TeV. We have shown that the LHCb data provided at the three CoM energies leads to consistent constraints on the small-x gluon. It is found that the combination of normalized cross section data available at the three CoM energies (namely $N_5 + N_7 + N_{13}$)
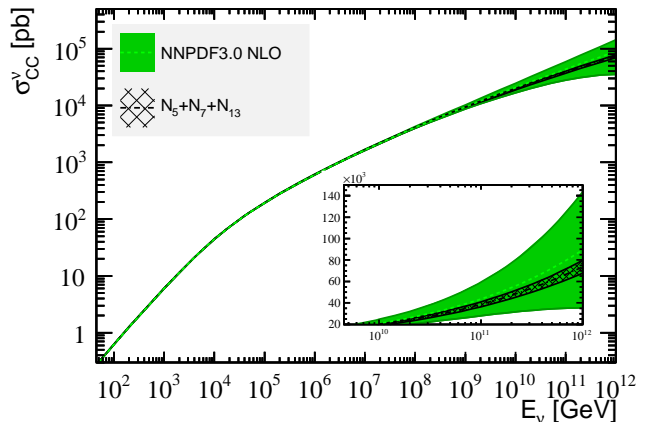

FIG. 6: The NLO charged-current neutrino-nucleus cross-section as a function of the neutrino energy E_ν, computed with NNPDF3.0 and with the results of this work.

leads to the strongest constraints on the low-x gluon PDF. While this result is shown to be reasonably stable upon theory variation (see Fig. 3), a future analysis at NNLO would also be desirable. Consistent results are also found when a combination of normalized cross-section and cross-section ratio data are included, the most constraining in this case being $N_7 + R_{13/5}$, and found to be robust with respect to theory variations. Our analysis provides a strong motivation to include the LHCb charm production data in the next generation of global PDF fits.

We have illustrated how the improved small-x gluon leads to significantly reduced theory uncertainties for F_L at future high-energy lepton-proton colliders and for the UHE neutrino-nucleus interactions. We have however only scratched the surface of the phenomenological implications of our work. It is important to explore these implications further to inform other applications, such as the modelling of semi-hard QCD processes at the LHC in Monte Carlo event generators and for calculations of cosmic ray production. Moreover, it would be interesting to compare our determination of the small-x gluon with those that could be achieved from other processes with similar kinematical coverage, such as exclusive production [48] or forward photon production [49, 50].

The results of this work are available upon request in the form of LHAPDF6 grids [34].

Comments regarding update of LHCb data. After completing our original analysis of the LHCb data in October 2016, it was pointed by one of us that there were a number of inconsistencies present in the heavy flavour production data provided by LHCb [51]. The charm cross-section measurements at 5 and 13 TeV [19, 20] were subsequently updated, and the current analysis includes these corrected data.

In our original analysis we observed tension between the NLO theory predictions and the LHCb data for N_5 and N_{13} observables in particular kinematic regions. In particular, this discrepancy was observed for rapidity bins which were farthest from the reference bin $y_{\rm ref}^D$ which normalises the cross section data, and at the time this was attributed to a limitation of the NLO theory predictions. Consequently, we applied a kinematic cut to restrict our analysis to exclude these regions. This tension is not observed in the update of the LHCb data, and no such kinematic restriction is applied in our analysis. It is likely we were observing the effects of the incorrect rapidity dependent efficiency correction which affected the LHCb data.

[1] S. Forte and G. Watt, Ann.Rev.Nucl.Part.Sci. **63**, 291 (2013), 1301.6754.
[2] J. Butterworth et al., J. Phys. **G43**, 023001 (2016), 1510.03865.
[3] J. Rojo et al., J. Phys. **G42**, 103103 (2015), 1507.00556.
[4] P. Skands, S. Carrazza, and J. Rojo, European Physical Journal **74**, 3024 (2014), 1404.5630.
[5] A. Cooper-Sarkar, P. Mertsch, and S. Sarkar, JHEP **08**, 042 (2011), 1106.3723.
[6] M. V. Garzelli, S. Moch, and G. Sigl, JHEP **10**, 115 (2015), 1507.01570.
[7] R. Gauld, J. Rojo, L. Rottoli, S. Sarkar, and J. Talbert, JHEP **02**, 130 (2016), 1511.06346.
[8] A. Bhattacharya, R. Enberg, Y. S. Jeong, C. S. Kim, M. H. Reno, I. Sarcevic, and A. Stasto (2016), 1607.00193.
[9] D. d'Enterria, R. Engel, T. Pierog, S. Ostapchenko, and K. Werner, Astropart. Phys. **35**, 98 (2011), 1101.5596.
[10] J. Abelleira Fernandez et al. (LHeC Study Group), J.Phys. **G39**, 075001 (2012), 1206.2913.
[11] M. L. Mangano et al. (2016), 1607.01831.
[12] H. Abramowicz et al. (H1 , ZEUS), Eur.Phys.J. **C73**, 2311 (2013), 1211.1182.
[13] H. Abramowicz et al. (ZEUS, H1), Eur. Phys. J. **C75**, 580 (2015), 1506.06042.
[14] R. Gauld, J. Rojo, L. Rottoli, and J. Talbert, JHEP **11**, 009 (2015), 1506.08025.
[15] O. Zenaiev et al. (PROSA), Eur. Phys. J. **C75**, 396 (2015), 1503.04581.
[16] M. Cacciari, M. L. Mangano, and P. Nason, Eur. Phys. J. **C75**, 610 (2015), 1507.06197.
[17] R. Aaij et al. (LHCb), Nucl.Phys. **B871**, 1 (2013), 1302.2864.
[18] M. L. Mangano and J. Rojo, JHEP **1208**, 010 (2012), 1206.3557.
[19] R. Aaij et al. (LHCb) (2016), 1610.02230.
[20] R. Aaij et al. (LHCb), JHEP **03**, 159 (2016), [Erratum: JHEP05,074(2017)], 1510.01707.
[21] R. D. Ball et al. (NNPDF), JHEP **1504**, 040 (2015), 1410.8849.
[22] M. Cacciari and M. Greco, Nucl.Phys. **B421**, 530 (1994), hep-ph/9311260.
[23] P. Nason, JHEP **0411**, 040 (2004), hep-ph/0409146.
[24] S. Frixione, P. Nason, and C. Oleari, JHEP **0711**, 070 (2007), 0709.2092.
[25] S. Alioli, P. Nason, C. Oleari, and E. Re, JHEP **1006**, 043 (2010), 1002.2581.
[26] S. Frixione, P. Nason, and G. Ridolfi, JHEP **0709**, 126 (2007), 0707.3088.
[27] T. Sjostrand, S. Mrenna, and P. Z. Skands, Comput. Phys. Commun. **178**, 852 (2008), 0710.3820.
[28] T. Sjöstrand, S. Ask, J. R. Christiansen, R. Corke, N. Desai, et al., Comput.Phys.Commun. **191**, 159 (2015), 1410.3012.
[29] M. Cacciari, S. Frixione, N. Houdeau, M. L. Mangano, P. Nason, et al., JHEP **1210**, 137 (2012), 1205.6344.
[30] S. Frixione and B. R. Webber, JHEP **0206**, 029 (2002), hep-ph/0204244.
[31] J. Alwall, R. Frederix, S. Frixione, V. Hirschi, F. Maltoni, et al., JHEP **1407**, 079 (2014), 1405.0301.
[32] M. Cacciari, M. Greco, and P. Nason, JHEP **9805**, 007 (1998), hep-ph/9803400.
[33] M. Cacciari, S. Frixione, and P. Nason, JHEP **0103**, 006 (2001), hep-ph/0102134.
[34] A. Buckley, J. Ferrando, S. Lloyd, K. Nordström, B. Page, et al., Eur.Phys.J. **C75**, 132 (2015), 1412.7420.
[35] D. de Florian et al. (The LHC Higgs Cross Section Working Group) (2016), 1610.07922.
[36] R. D. Ball et al. (The NNPDF), Nucl. Phys. **B849**, 112 (2011), 1012.0836.
[37] R. D. Ball, V. Bertone, F. Cerutti, L. Del Debbio, S. Forte, et al., Nucl.Phys. **B855**, 608 (2012), 1108.1758.
[38] M. Czakon, P. Fiedler, D. Heymes, and A. Mitov, JHEP **05**, 034 (2016), 1601.05375.
[39] V. Bertone, S. Carrazza, and J. Rojo, Comput.Phys.Commun. **185**, 1647 (2014), 1310.1394.
[40] S. Forte, E. Laenen, P. Nason, and J. Rojo, Nucl. Phys. **B834**, 116 (2010), 1001.2312.
[41] J. Rojo and F. Caola (2009), 0906.2079.
[42] M. G. Aartsen et al. (IceCube) (2016), 1607.05886.
[43] S. Adrian-Martinez et al. (KM3Net), J. Phys. **G43**, 084001 (2016), 1601.07459.
[44] R. D. Ball and S. Forte, Phys. Lett. **B335**, 77 (1994), hep-ph/9405320.
[45] J. L. Albacete, J. I. Illana, and A. Soto-Ontoso, Phys. Rev. **D92**, 014027 (2015), 1505.06583.
[46] A. Connolly, R. S. Thorne, and D. Waters, Phys. Rev. **D83**, 113009 (2011), 1102.0691.
[47] L. A. Anchordoqui et al., JHEAp **1-2**, 1 (2014), 1312.6587.
[48] S. P. Jones, A. D. Martin, M. G. Ryskin, and T. Teubner (2016), 1610.02272.
[49] D. d'Enterria and J. Rojo, Nucl.Phys. **B860**, 311 (2012), 1202.1762.
[50] T. Peitzmann (ALICE FoCal) (2016), 1607.01673.
[51] R. Gauld, JHEP **05**, 084 (2017), 1703.03636.